Lithos 125 (2011) 928–939

Contents lists available at ScienceDirect

Lithos

journal homepage: www.elsevier.com/locate/lithos

Geochemical variations in Miocene adakitic rocks from the western and eastern Lhasa terrane: Implications for lower crustal flow beneath the Southern Tibetan Plateau

Jian-Lin Chen [a], Ji-Feng Xu [a,*], Wen-Xia Zhao [b,*], Yan-Hui Dong [a], Bao-Di Wang [c], Zhi-Qiang Kang [d]

[a] State Key Laboratory of Isotope Geochemistry, Guangzhou Institute of Geochemistry, Chinese Academy of Sciences, Guangzhou 510640, China
[b] Instrumental Analysis and Research Center, Sun Yat-Sen University, Guangzhou 510275, China
[c] Chengdu Institute of Geology and Mineral Resources, Chengdu 610081, China
[d] Guilin University of Technology, Guilin 541004, China

ARTICLE INFO

Article history:
Received 4 October 2010
Accepted 21 May 2011
Available online 30 May 2011

Keywords:
Adakitic rocks
Mid-lower crust
Channel flow
Lhasa terrane
Tibetan Plateau

ABSTRACT

It is generally believed that Miocene adakitic rocks in the Lhasa terrane (block) of Southern Tibet were derived from a thickened lower crust, and that their compositions will therefore reflect the geochemical characteristics of their lower-crustal source(s). Adakitic rocks in the western part of the Lhasa terrane possess geochemical and Sr–Nd isotopic characteristics that are clearly different from those in the eastern part of the Lhasa terrane; the former display a more enriched Nd–Sr isotopic signature together with an older model age relative to the latter, suggesting that the compositions of the lower crust under the western and eastern parts of the Lhasa terrane also differ. In addition, the adakitic rocks in the Himalayas on the southern side of the Indus–Yalu suture (IYS) have similar geochemical characteristics and Sr–Nd isotopic compositions to the adakitic rocks of the western Lhasa terrane, but differ from rocks in the eastern Lhasa terrane and from igneous rocks derived from crust beneath the Himalayas. We suggest that the lower (and/or middle) crustal materials beneath the western Lhasa terrane probably extend to the southern side of the IYS due to channel flow. If mid-lower crustal flow has occurred below Southern Tibet, the southeastward-moving anatectic mid-lower crustal material was probably derived from below the western part of the Lhasa terrane rather than the eastern. Moreover, the emplacement ages of adakitic rocks from Mayum, on the southern side of the IYS, imply that southeastward ductile flow of mid-lower crust beneath western Lhasa may have occurred as early as 17 Ma.

© 2011 Elsevier B.V. All rights reserved.

1. Introduction

Geophysical studies have revealed similar geophysical anomalies in the mid-crust of the Lhasa terrane (block) and the Himalaya range (Nelson et al., 1996; Unsworth et al., 2005), and a channel flow model has been proposed to explain this phenomenon (Beaumont et al., 2001, 2004, 2006; Clark and Royden, 2000; Hodges, 2006; Hodges et al., 2001; Klemperer, 2006; Medvedev and Beaumont, 2006; Nelson et al., 1996). Based on a study of the Kuday dykes emplaced on the south side of the Indus–Yalu suture (IYS), King et al. (2007) proposed southward ductile flow of Asian crust beneath Southern Tibet. However, Harrison (2006) concluded that the southward flow was limited in extent because of the absence of Gangdese arc material on the south side of the IYS, and Leech (2008) suggested that the flow was interrupted by the Karakoram Fault in the western Himalayas. Therefore, the occurrence and nature of channel flow beneath Southern Tibet remain topics of controversy.

Miocene adakitic rocks in Southern Tibet are thought to have originated from a thickened lower crust (Cai et al., 2005; Chung et al., 2003, 2009; Gao et al., 2007a; Guo et al., 2007; Hou et al., 2004; Jiang et al., 2006), meaning that their compositions reflect the geochemical characteristics of their lower crustal source(s). Here, we present new geochemical data and Laser Ablation Inductively Coupled Plasma Mass Spectrometry (LA-ICP-MS) U–Pb zircon age data for adakitic rocks in the Lhasa terrane, which, when combined with previous geochemical data, allows us to assess possible sources on both sides of the IYS.

2. Background

The Tibetan Plateau is a tectonic collage of continental terranes or blocks. From north to south, the interior of the Tibetan Plateau comprises the roughly east–west-trending Songpan–Ganzi, Qiangtang, and Lhasa terranes (Dewey et al., 1988; Yin and Harrison, 2000). The Lhasa terrane is bounded by the Bangong–Nujiang Suture (BNS) to the north and the IYS to the south (Yin and Harrison, 2000) (Fig. 1). It is generally accepted that the BNS formed during the Late Jurassic–Middle Cretaceous (Yin and Harrison, 2000) and that the IYS formed

* Corresponding authors. Tel.: +86 20 8529 0282; fax: +86 20 8529 0130.
E-mail addresses: jifengxu@gig.ac.cn (J.-F. Xu), zhaowx@mail.sysu.edu.cn (W.-X. Zhao).

0024-4937/$ – see front matter © 2011 Elsevier B.V. All rights reserved.
doi:10.1016/j.lithos.2011.05.006

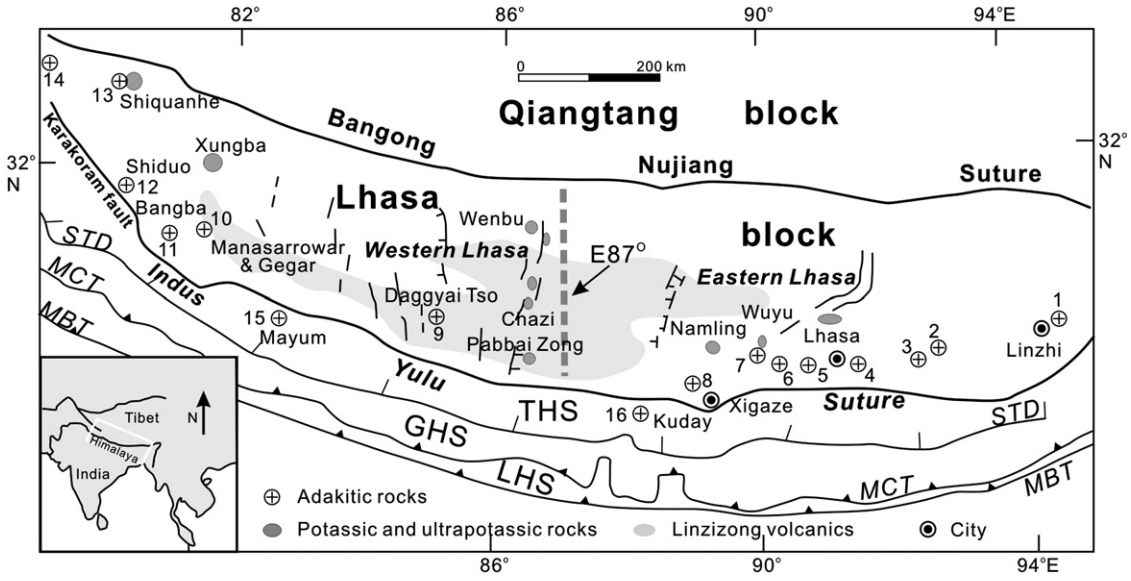

Fig. 1. Map showing sample localities and the occurrence of adakitic rocks in the Gangdese belt of southern Tibet, after Guo et al. (2007) and Gao et al. (2007a). The localities are as follows (from east to west): 1, Linzhi (Chung et al., 2003); 2, Jiama (Hou et al., 2004, the present study); 3, Qulong (Hou et al., 2004); 4, Lakang'e (Hou et al., 2004, the present study); 5, Nanmu (Hou et al., 2004); 6, Nemu (Hou et al., 2004, the present study); 7, Maquiang (Turner et al., 1996); 8, Xigaze (Chung et al., 2003); 9, Daggyaio Tso (Williams et al., 2004); 10, Manasarowar and Gegar (Miller et al., 1999); 11, Bangba (the present study); 12, Shiduo (Cai et al., 2005); 13, Shiquanhe (Guo et al., 2007); and 14, Ritu (Cai et al., 2005). The adakitic rocks in the Tethyan Himalayan tectonic zone are as follows: 15 Mayum (Jiang et al., 2006) and 16 Kuday (King et al., 2007). Also shown are the locations of potassic and ultrapotassic rocks. STD, Southern Tibetan Detachment; MCT, Main Central Thrust; MBT, Main Boundary Thrust; LHS, Lesser Himalayan Sequence; GHS, Greater Himalayan Sequence; THS, Tethyan Himalayan Sequence.

during the Late Cretaceous–Early Paleogene (Dewey et al., 1988). The IYS marks the closure of the Tethys, and lies immediately south of an extensive Andean-type calc-alkaline magmatic center (Linzizong volcanics and Gangdese batholith) in the Lhasa terrane (e.g., Coulon et al., 1986; Mo et al., 2008; Murphy et al., 1997; Scharer et al., 1984). Since its collision with Asia at 50 Ma, the ongoing northward movement of India has led to thickening of the Tibetan crust, which is now twice the thickness of normal crust (Owens and Zandt, 1997; Zhao and Nelson, 1993).

Volumetrically minor, post-collisional potassic–ultrapotassic rocks and adakitic rocks are widely distributed in the Lhasa terrane, and were produced at the end of subduction-related magmatism in Southern Tibet (Fig. 1). Previous studies have shown that the adakitic rocks are K-rich, forming a 1000-km-long belt oriented sub-parallel to the IYS. The ages of the adakitic rocks range from 26.2 to 10 Ma (Cai et al., 2005; Chung et al., 2003, 2009; Gao et al., 2007a; Guo et al., 2007; Hou et al., 2004; Xu et al., 2010; this study), within the range of the 22.5–12 Ma ages obtained for potassic–ultrapotassic igneous rocks in the Lhasa terrane (e.g., Ding et al., 2003; Gao et al., 2007b; Miller et al., 1999; Nomade et al., 2004; Williams et al., 2001, 2004; Zhao et al., 2009), except for the 26.2 Ma age of adakitic rocks in Linzhi (Chung et al., 2003). Recently, Miocene adakitic dykes have been found on the southern side of the IYS, including the Mayum and Kuday dykes (Jiang et al., 2006; King et al., 2007) within the northern belt of the Tethyan Himalayan tectonic zone. The data collected from outcrops of adakitic rocks are presented in Fig. 1. To identify spatial differences in geochemistry, adakitic rocks of the Lhasa terrane are divided into eastern and western groups, either side of the longitude of approximately 87°E (Fig. 1) (Guo et al., 2007; Hou et al., 2006; Xiao et al., 2007; Zhao et al., 2006, 2009; Zhou and Murphy, 2005).

The adakitic rocks of the Lhasa terrane consist of small-volume porphyries, dykes, plugs, and minor lava flows, which generally display a typical porphyritic texture. In the eastern Lhasa terrane, all the adakitic rocks occur as small intrusive bodies, consisting mainly of granitic porophyry, monzonitic granite porphyry, and quartz monzonitic porphyry. The main phenocryst phases (which make up 10%–35% of the rock mass) are plagioclase, amphibole, alkali feldspar, biotite, quartz, and minor clinopyroxene, with accessory zircon, apatite, and Fe–Ti oxides. The groundmasses of these porphyries consist mainly of plagioclase, alkali feldspar, biotite, quartz, zircon, Fe–Ti oxides, titanite, apatite, and glass. The petrographic characteristics of these adakitic rocks have been described by Hou et al. (2004), Guo et al. (2007), and Gao et al. (2007a, 2007b). In the western Lhasa terrane, the adakitic rocks occur as erupted lavas or small intrusive bodies. These adakitic lavas have only been found in the western Lhasa terrane; e.g., at Bangba, such lavas are vesicular and porphyritic. Phenocrysts within the lavas include plagioclase, alkali feldspar, and biotite; the groundmass is cryptocrystalline. The petrographic characteristics of adakitic intrusive rocks in the western Lhasa terrane are similar to those in the eastern Lhasa terrane.

3. Analytical techniques

All samples were cleaned of weathered surfaces prior to being powdered in an agate ring mill for analyses of major and trace elements, and Sr–Nd isotopes, performed at the Guangzhou Institute of Geochemistry, Chinese Academy of Sciences (GIGCAS), Guangzhou, China.

Major elements were measured using an X-ray fluorescence spectrometer (XRF) on glass disks, following the analytical procedures described by Goto and Tatsumi (1996). A 900 °C pre-ignition was used to determine the loss on ignition (LOI) prior to major element analyses. Analyses of Chinese standard reference materials (GSR-1, GSR-2 and GSR-3) indicate that analytical uncertainties for major elements were generally better than 5% (Appendix 1). Trace-element data were obtained using inductively coupled plasma-mass spectrometry (ICP-MS) techniques, following the analytical procedures described by Chen et al. (2010). The precision for rare earth elements (REEs) and high field strength elements (HFSEs) is estimated to be 5%, based on analyses of the USGS and Chinese standards BHVO-2, AGV-1, GSR-1, and W-2 (Appendix 2).

Sr and Nd isotopic compositions were measured using a Micromass Isoprobe multi-collector-inductively coupled plasma-mass spectrometer (MC-ICP-MS) and a Triton Thermal Ionization Mass

Spectrometry (TIMS) at GIGCAS. Analytical procedures for Sr and Nd isotopes are described in detail by Li et al. (2004), Wei et al. (2002), and Chen et al. (2010). The method of chemical separation of Sr and Nd was similar to that described by Li and McCulloch (1998), Xu et al. (2002), and Chen et al. (2010). Isotopic data for the samples from Bangba were obtained using MC-ICP-MS; all the other samples were analyzed using Triton TIMS. The $^{87}Sr/^{86}Sr$ value of the NBS987 standard and the $^{143}Nd/^{144}Nd$ value of the JNdi-1 standard were 0.710288 ± 28 (2σ) and 0.512109 ± 12 (2σ), respectively; fractionation corrections of $^{146}Nd/^{144}Nd = 0.7219$ and $^{86}Sr/^{88}Sr = 0.1194$ were applied to all measured $^{143}Nd/^{144}Nd$ and $^{86}Sr/^{88}Sr$ values, respectively.

Zircons for LA-ICP-MS U–Pb dating were extracted using conventional heavy liquid and magnetic techniques, and individually selected by hand-picking under a binocular microscope. They were mounted in epoxy resin and polished for subsequent cathodoluminescence (CL) observations and LA-ICP-MS analysis. Zircon U–Pb analyses of samples from the Bangba, Nemu, and Jiama areas were performed at the LA-ICP-MS Laboratory in the Department of Earth and Planetary Sciences, Macquarie University, Australia. Analytical procedures followed those described by Griffin et al. (2002) and Xu et al. (2003) for zircon analysis using LA-ICP-MS.

4. Age data and geochemistry

4.1. Chronology

LA-ICP-MS zircon U–Pb data (Appendix 3) shown in Fig. 2. The CL images of zircon show regular oscillatory magmatic zoning with no resorption cores; Th/U ratios range from 0.12 to 2.14. These ratios are higher than those of metamorphic zircons, which generally yield values of <0.1; however, they are consistent with values obtained for magmatic zircons (Williams et al., 1996).

The results of LA-ICP-MS zircon U–Pb analyses for three samples from the Nemu and Jiama areas in the eastern Lhasa terrane (NM03-01, JM03-05, and JM03-06) and one sample from the Bangba area in the western Lhasa terrane (07BB-03) are shown on a concordia plot in Fig. 2. The 8 analyses for sample NM03-01, 10 analyses for sample JM03-05, 10 analyses for sample JM03-06, and 17 analyses for sample 07BB-03 define single age populations with a weighted mean $^{206}Pb/^{238}U$ ages of 12.75 ± 0.19 Ma (2σ) (MSWD = 1.20), 15.50 ± 0.14 Ma (2σ) (MSWD = 0.71), 15.46 ± 0.20 Ma (2σ) (MSWD = 1.9), and 17.01 ± 0.23 Ma (2σ) (MSWD = 2.0), respectively (Fig. 2). These results are consistent with the age data reported by Chung et al. (2003) and Hou et al. (2004).

4.2. Major and trace element geochemistry

The major and trace element data obtained for igneous rocks from the western and eastern parts of the Lhasa terrane (Table 1), as well as previously published data from both sides of the IYS (Fig. 1), show a calc-alkaline and high-K series affinity in the SiO_2 vs. $Na_2O + K_2O$ (TAS) plot (Fig. 3) and on the K_2O vs. SiO_2 plot (Fig. 4). In major-element Harker diagrams (Fig. 5), the samples from western Lhasa have relatively high CaO, Fe_2O_3, MgO and TiO_2 concentrations, and similar Al_2O_3 and Na_2O concentrations to those from the eastern Lhasa terrane. The adakitic samples on the south side of the IYS have similar characteristics to those from the western Lhasa terrane.

Chondrite-normalized REE patterns for all samples (Fig. 6a) show clear fractionation between light REEs (LREEs) and heavy REEs (HREEs); no significant negative Eu anomalies are found. The samples

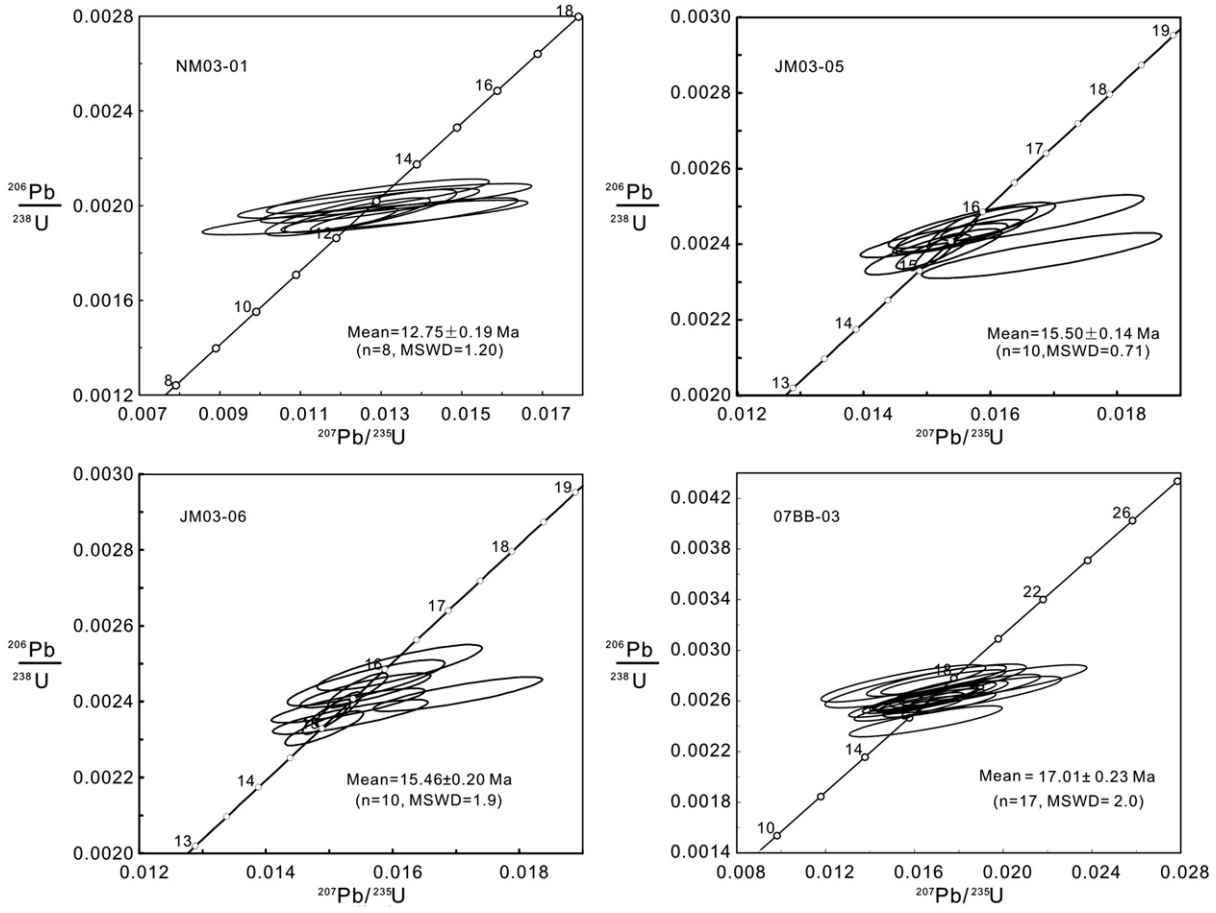

Fig. 2. LA-ICP-MS U–Pb concordia diagram for samples NM03-01, JM03-05, JM03-06, and 07BB-03.

Table 1
Major (wt.%) and trace element (ppm) concentrations for adakitic rocks of the southern Lhasa terrane.

Sample	07BB-02	07BB-03	07BB-04	07BB-06	07BB-07	NM03-1	NM03-2	NM03-3	NM03-4	JM03-4	JM03-5	LKE03-02
Location	Bangba					Nemu				Jiama		Lakang'e
	Western of Lhasa					Eastern of Lhasa						
SiO_2	63.38	62.34	62.28	69.44	68.10	72.46	69.99	67.36	66.95	70.42	68.95	69.95
TiO_2	0.89	0.88	0.90	0.64	0.56	0.24	0.35	0.29	0.47	0.38	0.60	0.51
Al_2O_3	16.65	15.89	16.30	14.38	17.28	14.04	14.63	15.80	16.78	15.76	15.53	15.53
Fe_2O_3	5.20	5.50	5.48	3.14	2.22	1.66	3.24	4.60	3.42	1.80	1.31	2.49
MnO	0.05	0.05	0.05	0.03	0.03	0.01	0.02	0.02	0.01	0.02	0.02	0.04
MgO	1.65	2.30	2.26	0.99	1.39	0.40	0.99	1.05	1.28	0.89	1.19	1.73
CaO	3.54	4.14	4.08	2.12	1.54	0.56	1.33	1.30	0.69	4.42	1.07	0.91
Na_2O	3.19	3.29	3.17	3.32	2.11	3.92	3.79	3.85	4.68	1.68	4.50	3.71
K_2O	3.60	3.84	3.71	4.41	5.34	4.00	3.50	3.71	3.07	3.27	5.19	3.86
P_2O_5	0.28	0.33	0.37	0.30	0.12	0.05	0.05	0.05	0.04	0.08	0.02	0.02
LOI	1.50	1.23	1.25	0.97	1.32	1.90	1.50	1.74	2.99	1.08	1.39	1.33
Total	99.92	99.80	99.86	99.74	99.99	99.24	99.39	99.77	100.38	99.80	99.77	100.07
Sc	12.06	13.02	14.16	6.05		1.38	2.71	3.58	3.40	1.92	5.07	5.19
V	122	114.7	122	66.68		35.53	63.66	41.67	65.63	48.91	63.96	68.18
Cr	77.72	72.37	77.10	29.77		28.79	18.46	25.12	16.77	15.77	35.61	64.48
Co	14.31	16.28	16.14	6.59		4.06	4.34	8.15	7.65	5.90	3.56	7.12
Ni	39.78	45.85	40.89	15.91		8.15	9.99	12.86	9.77	8.79	14.96	30.17
Rb	127	142	147	217		132	117	133	143	143	252	97.87
Ba	1795	1752	1907	1472		705	731	670	696	490	661	1085
Th	18.78	21.34	21.35	46.21		8.09	5.93	8.98	7.78	16.99	12.56	9.34
U	3.28	3.72	3.33	10.17		2.59	1.73	1.89	2.86	4.32	5.29	3.66
Nb	8.96	8.66	8.73	10.95		4.45	3.47	3.65	3.30	5.71	5.67	4.68
Ta	0.60	0.57	0.58	0.80		0.30	0.26	0.31	0.23	0.49	0.40	0.35
La	42.53	48.62	53.62	36.72		12.92	14.18	8.52	12.20	25.60	29.18	11.03
Ce	85.68	102	112	75.42		24.77	28.09	16.98	25.88	47.71	56.64	22.26
Pb	36.55	34.76	36.48	44.17		15.95	19.69	22.00	9.57	24.43	12.69	16.84
Pr	11.20	12.75	13.69	10.15		3.54	3.33	2.05	3.27	5.55	6.94	2.63
Sr	1030	1239	1283	586		337	641	579	658	360	330	715
Nd	43.21	50.28	52.84	41.76		12.90	12.03	7.46	12.50	18.99	24.67	9.35
Zr	231	227	230	171		84.30	90.04	96.10	110	104	130	123
Hf	6.97	6.63	6.87	5.42		2.49	2.51	2.72	2.90	3.13	3.58	3.63
Sm	7.53	8.75	9.04	8.33		2.15	1.78	1.22	2.25	2.94	3.82	1.50
Eu	1.84	2.07	2.14	1.55		0.40	0.43	0.29	0.52	0.81	0.82	0.27
Gd	5.21	6.12	6.15	5.30		1.27	1.06	0.72	1.39	1.70	2.20	0.94
Tb	0.60	0.75	0.71	0.62		0.16	0.14	0.10	0.18	0.23	0.27	0.13
Dy	2.93	3.65	3.42	2.84		0.72	0.69	0.54	0.88	1.17	1.29	0.72
Y	13.02	17.47	15.51	12.53		3.77	3.60	3.05	4.28	6.37	5.96	3.77
Ho	0.50	0.64	0.58	0.45		0.13	0.13	0.11	0.16	0.22	0.21	0.14
Er	1.28	1.69	1.47	1.22		0.35	0.36	0.31	0.43	0.59	0.57	0.38
Tm	0.18	0.21	0.20	0.17		0.05	0.05	0.05	0.07	0.09	0.09	0.07
Yb	1.07	1.39	1.28	1.06		0.39	0.39	0.40	0.50	0.67	0.59	0.49
Lu	0.17	0.22	0.20	0.16		0.07	0.07	0.08	0.08	0.12	0.10	0.09

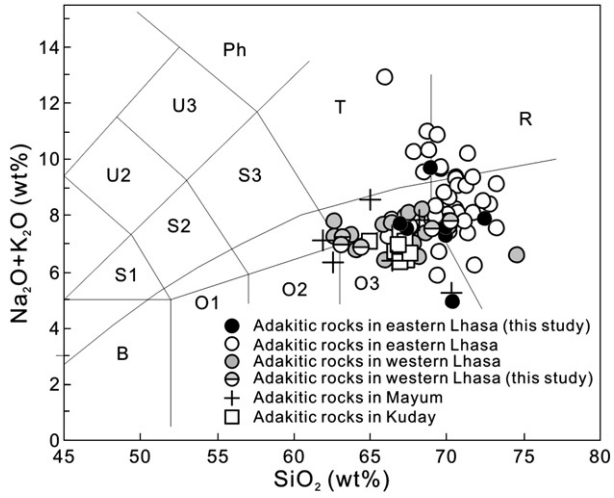

Fig. 3. TAS diagram showing data for adakitic rocks from Southern Tibet (from Le Bas et al., 1986). Data sources are as in Fig. 1. Rock types are indicated by letters, as follows: B, basalt; O1, basaltic andesite; O2, andesite; O3, dacite; R, rhyolite; S1, trachybasalt; S2, basaltic trachyandesite; S3, trachyandesite; T, trachyte; U2, phonotephrite; U3, tephriphonolite; Ph, phonolite.

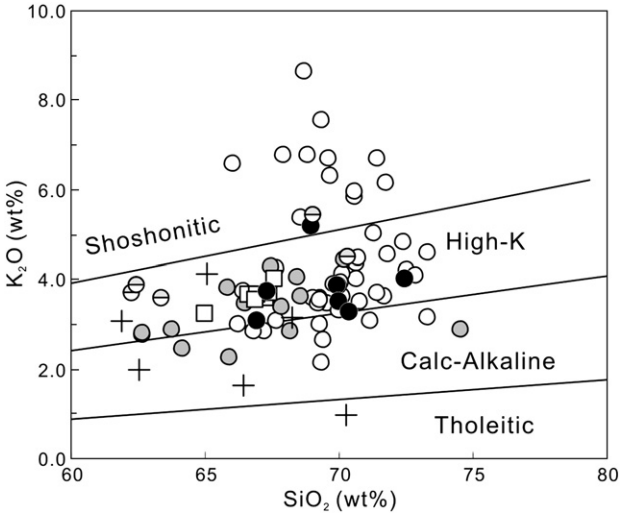

Fig. 4. SiO_2 vs. K_2O diagram for adakitic rocks in Southern Tibet (data sources and symbols are as in Figs. 1 and 3).

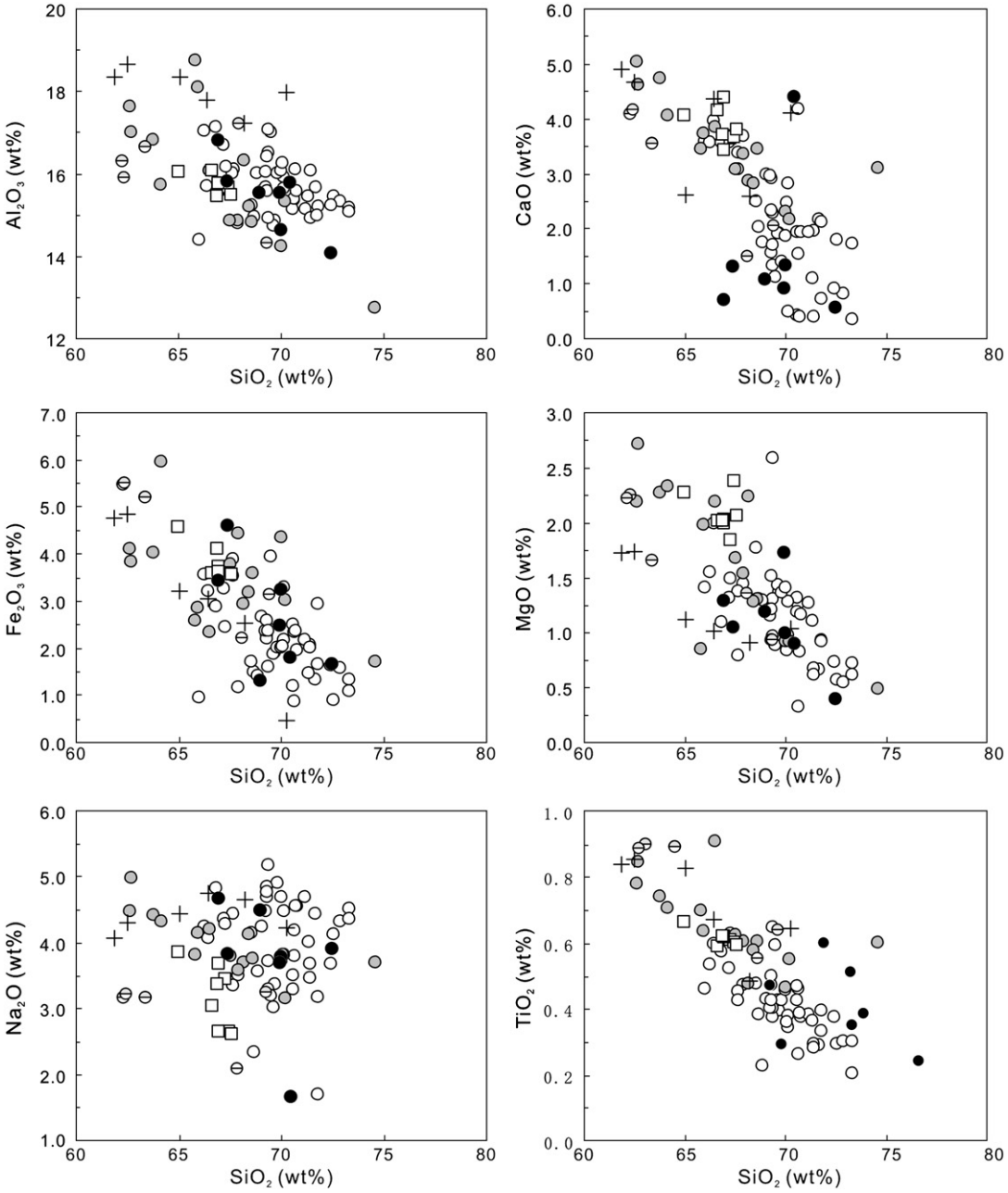

Fig. 5. Harker diagrams of major element concentrations vs. SiO_2 for adakitic rocks in Southern Tibet (data sources and symbols are as in Figs. 1 and 3).

from the western Lhasa terrane have higher REE concentrations than those from the eastern Lhasa terrane; and the samples on the south side of the IYS have similar patterns to those from the western Lhasa terrane.

A primitive mantle-normalized trace-element spider diagram for all samples (Fig. 6b) shows strong enrichment in large ion lithophile elements (LILEs) (e.g., Rb, Th, and U) relative to the HFSEs, and pronounced negative Nb–Ta–Ti anomalies. Compared with the samples of the eastern Lhasa terrane, those from the western Lhasa terrane have higher concentrations of trace elements, including Sr, Zr, La, Y, and Yb (Figs. 6b and 7), similar to the samples from the south side of the IYS.

4.3. Sr–Nd isotope geochemistry

The Sr–Nd isotopic data (Table 2), combined with previously published data from both sides of the IYS, show that the samples from the western Lhasa terrane are clearly different to those from the eastern Lhasa terrane; i.e., the former generally show lower εNd (T) values (−4.97 to −10.58) (Fig. 8) than the latter (−3.52 to 5.52, except for −6.18 in one sample). Therefore, samples from the western Lhasa terrane show an enriched Sr–Nd isotopic signature relative to those from the eastern Lhasa terrane. The isotopic signature of the samples from the western Lhasa terrane is considered to be analogous to that of samples from the south side of the IYS (Jiang et al., 2006; King et al., 2007) (except for one Mayum sample with εNd (T) = 3.53).

4.4. Characteristics of adakitic rocks

The major and trace element data for igneous rocks from both sides of the IYS display adakitic compositional affinities. They are intermediate to acidic in composition ($SiO_2 \geq 59$ wt.%), and have high Al_2O_3 (14–19 wt.%) and low MgO (<3.0 wt.%). These characteristics, combined with high Sr/Y, high LREE/HREE ratios, low HREEs contents,

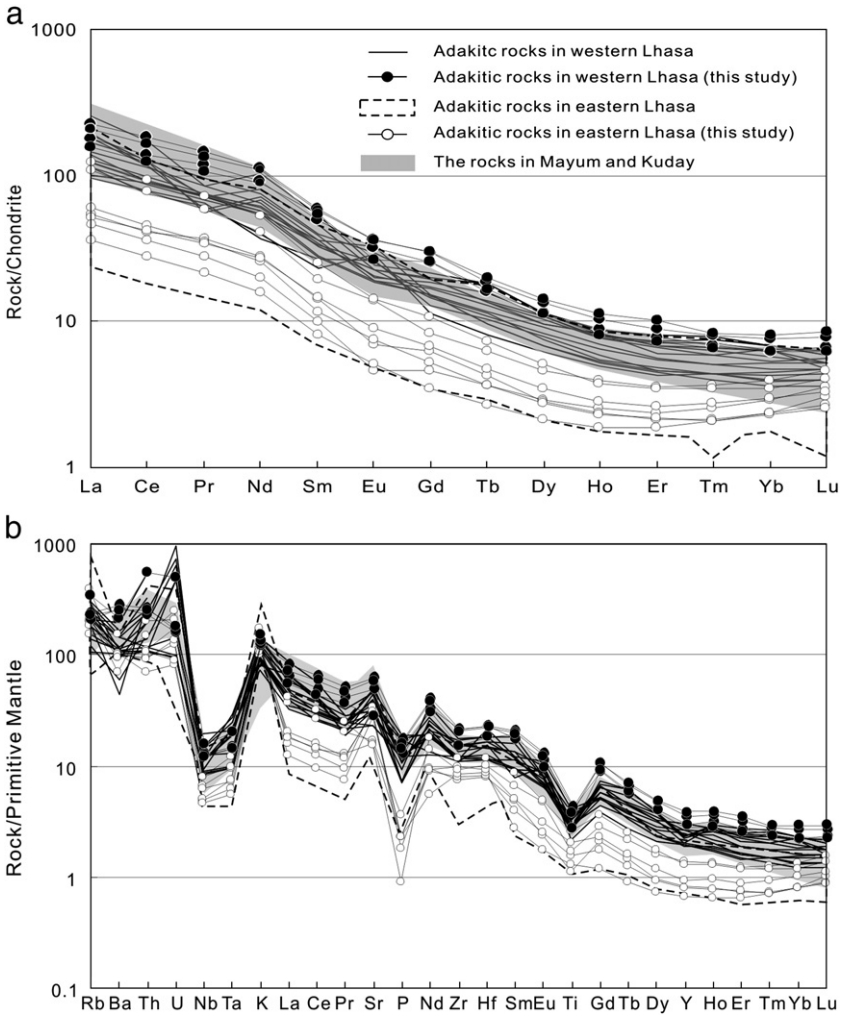

Fig. 6. Chondrite-normalized REE (a) and multi-element patterns normalized to primitive mantle (b) for adakitic rocks in Southern Tibet. Normalizing values are from Sun and McDonough (1989). Data sources are as in Fig. 1.

depleted HFSEs, and the lack of an obvious negative Eu anomaly, are distinctive features of adakites in subduction-zone settings (Defant and Drummond, 1990; Kay et al., 1993) (Fig. 9). These geochemical features are consistent with a magmatic origin from partial melting of garnet and rutile-bearing mafic source rocks (Xiong et al., 2005), which existed in the lower part of the collision-thickened Tibetan crust (Chung et al., 2003, 2009; Guo et al., 2007; Hou et al., 2004).

5. Discussion

5.1. Origin of the adakitic rocks: partial melting of lower crust

Three models commonly invoked to explain the genesis of adakitic rocks are slab melting, assimilation and fractional crystallization (AFC), and the melting of delaminated lower crust. However, none of these models appears to provide a tenable explanation for the genesis of the adakitic rocks of Southern Tibet. First, the Miocene adakitic rocks in Southern Tibet are found in the interior of a continent setting, which is inconsistent with a simple model of slab melting in an arc setting (Guo et al., 2007). Second, although these adakitic rocks are spatially and temporally associated with ultrapotassic rocks, they have Sr–Nd isotope compositions that distinguish them from the ultrapotassic rocks, suggesting an origin incompatible with the AFC model of ultrapotassic magma generation (Gao et al., 2007a, 2007b; Guo et al., 2007). Third, most adakitic rocks in Southern Tibet have relatively low contents of Cr, Ni, and other compatible elements, which is inconsistent with a model of melting involving delaminated lower crust (Xu et al., 2002).

Chung et al. (2003), Hou et al. (2004), and Guo et al. (2007) proposed that adakitic rocks in Southern Tibet were produced by partial melting of a thickened lower crust. The present data for adakitic rocks are consistent with the geochemical and Sr–Nd isotope characteristics of adakitic rocks derived from a lower crust source(s), as documented in previous studies. Therefore, we support the idea that the Miocene adakitic rocks were formed by partial melting of lower crust beneath Southern Tibet.

5.2. Compositional differences between the lower crust beneath west and east Lhasa

As mentioned above, the Miocene adakitic rocks display high Sr/Y, high LREE/HREE ratios, depleted HFSEs, and an absence of obviously negative Eu anomalies, indicating that the adakitic groups in both the western and eastern Lhasa terranes were the products of partial melting of thickened mafic lower crust (Chung et al., 2003, 2009; Guo et al., 2007; Hou et al., 2004). However, the geochemistry of adakitic rocks in the eastern Lhasa terrane is different from that of adakitic rocks in the western Lhasa terrane; this difference is seen for major and trace element concentrations and ratios (Figs. 5, 6, 7, and 9), suggesting that both crustal sources were heterogeneous. Most

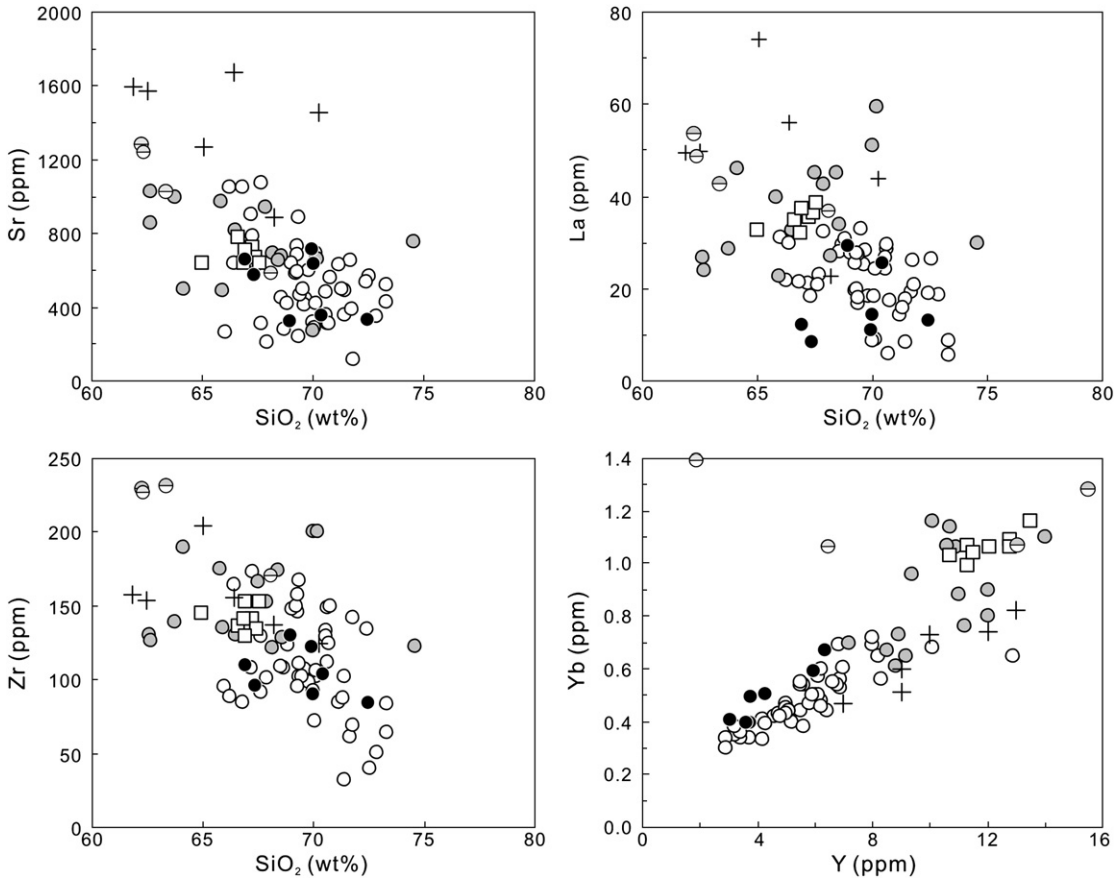

Fig. 7. Plots of SiO_2 vs. trace element concentrations, and Y vs. Yb for adakitic rocks in Southern Tibet (data sources and symbols are as in Figs. 1 and 3).

importantly, the adakitic rocks in the western Lhasa terrane have much lower εNd (T) values (−5 to −10) and older Nd model ages (T_{DM} = 1.1–1.8 Ga, average value: 1.4 Ga) compared with the eastern Lhasa terrane (εNd (T) = 5.5 to −3.5 (except for one value of −6.2); T_{DM} = 0.3–1.0 Ga, average value: 0.71 Ga) (Figs. 8 and 10a), indicating that the lower crust beneath the western Lhasa terrane is older and enriched relative to that under the eastern Lhasa terrane.

Considering that the ultrapotassic lavas which are temporally and spatially associated with the adakitic rocks are only exposed west of longitude 87°E, whereas potassic lavas are exposed both east and west of this longitude (Zhao et al., 2006, 2009) (Fig. 1), Guo et al. (2007) suggested that the different geochemical and Sr–Nd isotope compositions of adakitic rocks in the eastern and western Lhasa terranes are the result of mixing between ultrapotassic magmas and lower crustal melts beneath the Lhasa terrane. Accordingly, the adakitic rocks in the western Lhasa terrane should display higher K_2O and K_2O/Na_2O values than those from the eastern Lhasa terrane (Gao et al., 2010), corresponding to other transitional characteristics, such as K_2O concentrations and older Nd model ages between the Miocene ultrapotassic rocks and the adakitic rocks in western Lhasa. However, these regional characteristics are not seen (Figs. 4, and 10a). In addition, the adakitic rocks in the western Lhasa terrane show no evidence of compositional mixing in a plot of $^{87}Sr/^{86}Sr_{(i)}$ vs. 1000/Sr (Fig. 10b).

Xu et al. (2010) proposed that adakitic magmas in the Lhasa terrane were produced by mixing between melt derived from subducted Indian mafic lower crust in the Himalaya terrane and ultrapotassic lava in the

Table 2
Results of Sr–Nd isotope analyses of adakitic rocks in the southern Lhasa terrane.

Sample	07BB-04	NM03-1	NM03-2	NM03-3	NM03-4	JM03-4	JM03-5	LKE03-2
Age (Ma)[a]	17.01	12.8				15.5		13.4
Rb (ppm)	147	132	117	133	143	143	252	97.87
Sr (ppm)	1283	337	641	579	658	360	330	715
$^{87}Rb/^{86}Sr$	0.33059	1.13390	0.52766	0.66692	0.62912	1.14478	2.21314	0.39624
$^{87}Sr/^{86}Sr$	0.708019	0.705457	0.705256	0.705364	0.705214	0.708828	0.707260	0.705603
2σ	0.000013	0.000006	0.000005	0.000006	0.000007	0.000005	0.000005	0.000006
$(^{87}Sr/^{86}Sr)_i$	0.707920	0.705216	0.705144	0.705122	0.705102	0.708584	0.706788	0.705528
Sm (ppm)	9.04	2.15	1.78	1.22	2.25	2.94	3.82	1.50
Nd (ppm)	52.84	12.90	12.03	7.46	12.50	18.99	24.67	9.35
$^{147}Sm/^{144}Nd$	0.10343	0.10085	0.08950	0.09885	0.10887	0.09347	0.09361	0.09702
2σ	0.000011	0.000006	0.000005	0.000004	0.000005	0.000005	0.000006	0.00006
$(^{143}Nd/^{144}Nd)_i$	0.512349	0.512584	0.512594	0.512586	0.512621	0.512562	0.512434	0.512604
εNd(T)	−5.11	−0.67	−0.47	−0.65	0.05	−1.11	−3.61	−0.33
T_{DM}(Ga)	1.09	0.75	0.67	0.75	0.64	0.74	0.90	0.71

[a] Age data for adakitic rocks at Bangba, Nemu, and Jiama are from this study; age data for adakitic rocks at Lakang'e are from Qu et al. (2003).

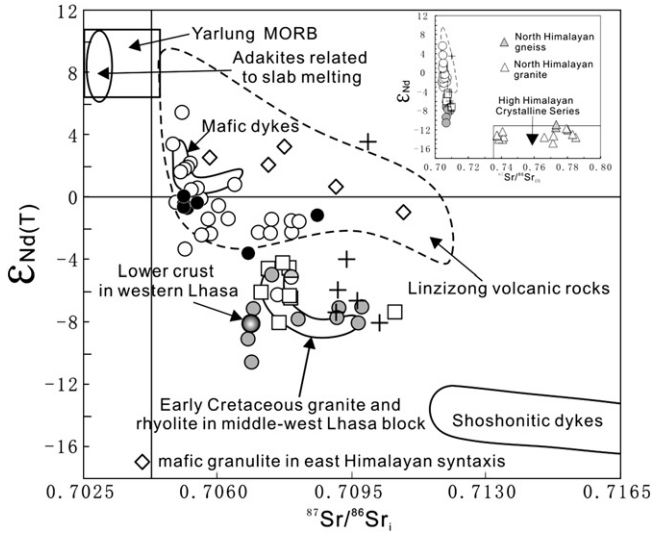

Fig. 8. $^{87}Sr/^{86}Sr_{(i)}$ vs. εNd(T) diagram for adakitic rocks and other rocks in Southern Tibet. Data sources are as follows: mafic dykes and Linzizong volcanic rocks are from Mo et al. (2008) and Yue and Ding (2006); Yarlung MORB is from Miller et al. (2003), Mahoney et al. (1998), Xu and Castillo (2004), and Zhang et al. (2005); lower crust in the western Lhasa terrane is from Miller et al. (1999); Shoshonitic dykes are from Zhao et al. (2009); adakites related to slab melting are from Kay (1978), Kay et al. (1993), and Stern and Kilian (1996); Early Cretaceous granite and rhyolites in the western Lhasa terrane are from Zhu et al. (2009); Northern Himalayan gneiss and granites are from Zhang et al. (2004); High Himalayan Crystalline Series is from Harris et al. (1988); mafic granulite in the east Himalayan syntaxis is from Xu et al. (2010) (other data sources and symbols are as in Figs. 1 and 3).

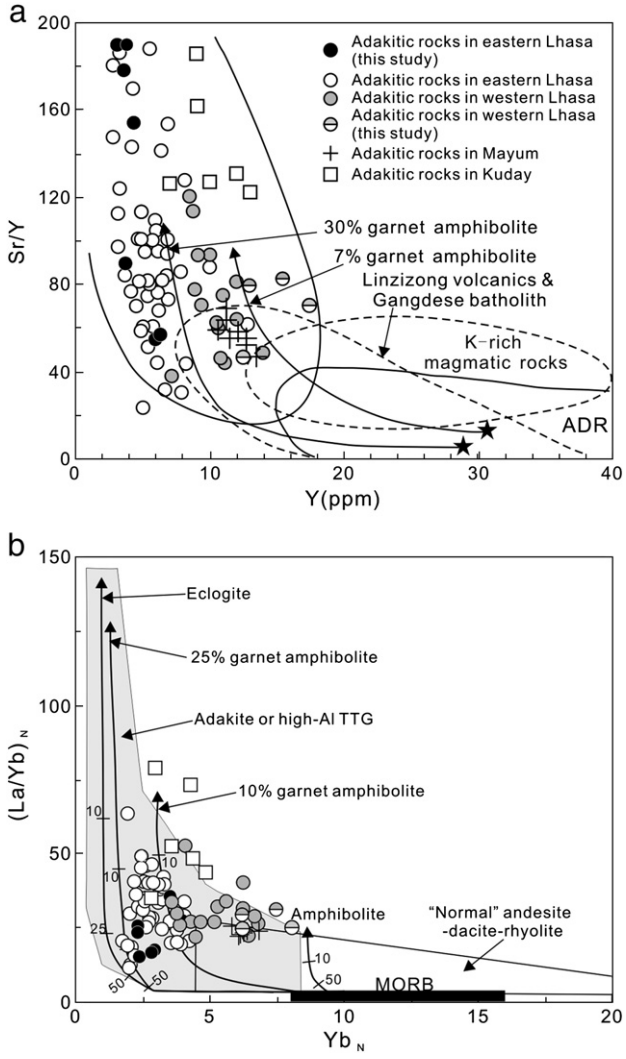

Fig. 9. (a) Sr/Y vs. Y plots after Drummond and Defant (1990) and Martin (1986), and (b) La_N/Yb_N vs. Yb_N after Defant and Drummond (1990) and Petford and Atherton (1996), showing the fields for adakite and arc intermediate-felsic rock. Data sources are as follows: Linzizong volcanics and the Gangdese batholith are from Zhang (1996), Jiang et al. (1999), Song (1999), and Wu et al. (2005); K-rich magmatic rocks are from Miller et al. (1999), Williams et al. (2001, 2004), Ding et al. (2003), Nomade et al. (2004), and Gao et al. (2007b) (other data sources are as in Figs. 1 and 3).

Lhasa terrane, which is similar to the concept proposed by Zhao et al. (2009). However, this idea is inconsistent with some of the geochemical characteristics of the adakitic rocks in the Lhasa terrane. First, while the adakitic lavas in the Lhasa terrane were erupted alone or with ultrapotassic and potassic lavas, they have different Sr–Nd isotope compositions to the ultrapotassic and potassic rocks (Chung et al., 2003; Guo et al., 2007; Hou et al., 2004; Miller et al., 1999; Zhao et al., 2009), which implies that they have different sources. Second, as discussed above, some adakitic rocks, such as those in the western Lhasa terrane, do not show these mixing characteristics. Third, Xu et al. (2010) reported that the melting of mafic granulites in the Himalaya terrane results in relatively low K_2O concentrations, which are inconsistent with the high K_2O content of adakitic rocks in the Lhasa terrane. In addition, based on the Sr–Nd isotope composition of adakitic rocks in the Lhasa terrane, Gao et al. (2010) considered that the mafic granulite in the Himalaya terrane is unlikely to be a non-radiogenic end-member for the mixing array in the Sr–Nd plot. Finally, the adakitic rocks in the Lhasa terrane have different Sr–Nd isotopic characteristics to the gneiss and granites of the North Himalayan (Zhang et al., 2004) and High Himalayan Crystalline Series (Harris et al., 1988), which have anomalously enriched Sr–Nd isotopic compositions relative to the adakitic rocks (Fig. 8). These results suggest that the crust beneath the Himalayan area was not the source of the adakitic rocks in the Lhasa terrane.

The geochemical differences between the adakitic rocks in the western and eastern Lhasa terranes are unlikely to have been caused by mixing between ultrapotassic magma and melt from the lower crust below the Lhasa terrane, or with mafic lower crust of the subducted Indian Plate (Xu et al., 2010; Zhao et al., 2009). On the other hand, these distinctive geochemical characteristics of the adakitic rocks in the western and eastern Lhasa terranes probably indicate compositional heterogeneities in the lower crust within this region. Moreover, the adakitic rocks in western Lhasa show Sr–Nd isotope values and Nd model ages that are similar to those of Early Cretaceous (110 ± 3 Ma) granites and rhyolites (T_{DM} = 1.2–1.5 Ga) in the central Lhasa subterrane (Zhu et al., 2009), which are considered to be the ancient basement of a micro-continental block that extends E–W for >700 km (82°E–89°E) (Zhu et al., 2009). This interpretation is consistent with the existence of a systematic compositional difference between the western and eastern parts of the lower crust beneath the Lhasa terrane (Hou et al., 2006; Zhao et al., 2009).

5.3. Origin of adakitic rocks on the south side of the IYS

Miocene adakitic rocks in Southern Tibet were previously thought to be exposed only in the Lhasa terrane, but adakitic rocks have recently been identified at two locations in the Himalayas. Jiang et al. (2006) reported the Mayum adakitic porphyry in the Himalayas on the southern side of the IYS. Subsequently, King et al. (2007) described the Miocene Kuday dykes on the southern side of the IYS, which are also depleted in HREEs and have high Sr/Y ratios, similar to the adakites. Chung et al. (2009) suggested that the Kuday dykes were derived from the lower crust. As discussed above, the Kuday and Mayum rocks have geochemical characteristics similar to the adakitic

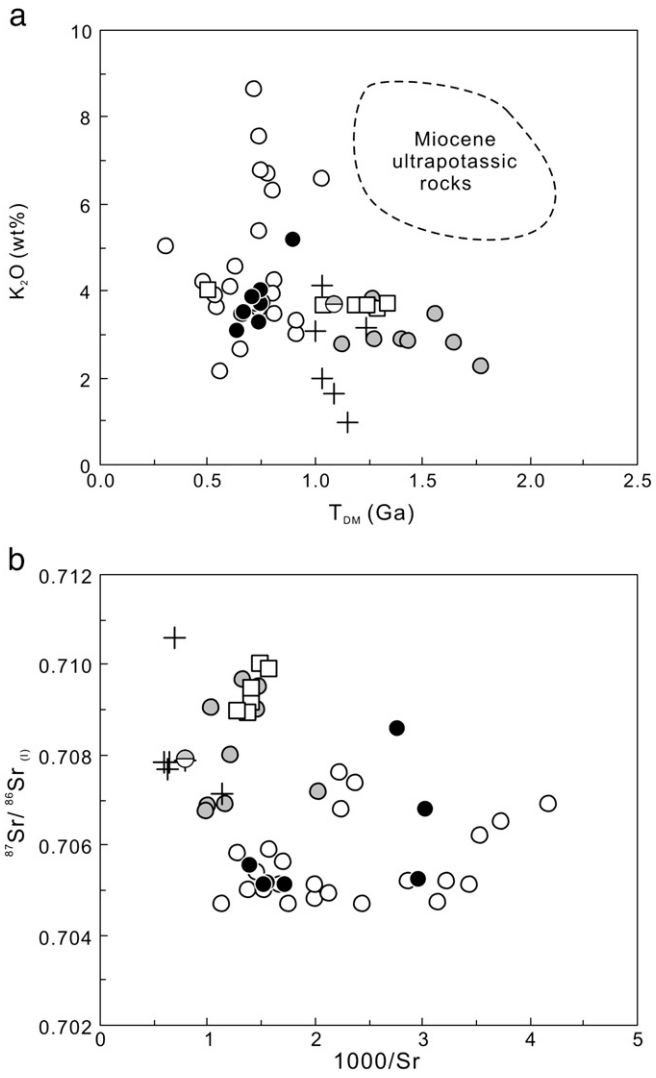

Fig. 10. Plots of T_{DM} (Ga) vs. K_2O (a) and 1000/Sr vs. $^{87}Sr/^{86}Sr_{(i)}$ (b) for adakitic rocks in Southern Tibet. Data for Miocene ultrapotassic rocks in the Lhasa terrane are from Miller et al. (1999), Williams et al. (2004), Gao et al. (2007b), and Zhao et al. (2009). Other data sources and symbols are as in Figs. 1 and 3.

rocks in the Lhasa terrane (Figs. 5–9), indicating that they too may have been generated by partial melting of a thickened lower crust.

It remains unclear how the Miocene Kuday and Mayum adakitic rocks were formed and why they occur south of the IYS. One possibility is that they were derived directly from lower crust beneath the Tethyan Himalayan area. However, as shown in Fig. 8, the Kuday and Mayum adakitic rocks display different Sr–Nd isotopic characteristics to gneiss and granites of the North Himalayan (Zhang et al., 2004) and High Himalayan Crystalline Series (Harris et al., 1988), which have anomalously enriched Sr–Nd isotopic compositions relative to the adakitic rocks, suggesting that the crust beneath the Himalayan area was not the source for the Kuday and Mayum adakitic rocks (King et al., 2007).

King et al. (2007) suggested that the Kuday dykes were produced by partial melting of Asian crustal material that had been moved southward by ductile flow, from below the eastern part of the Lhasa terrane to a new position beneath the Tethyan Himalayas. However, the adakitic rocks from the eastern Lhasa terrane and the Kuday adakitic rocks have contrasting trace element and Sr–Nd isotopes, indicating that the eastern Lhasa crust was not the magmatic source of the Kuday adakitic rocks. On the other hand, the Kuday and Mayum adakitic rocks have similar trace element and Sr–Nd isotope characteristics to those of the adakitic rocks, and to lower-crustal xenoliths (Miller et al., 1999) and Early Cretaceous (110 ± 3 Ma) granites and rhyolites (Zhu et al., 2009) from the western Lhasa terrane (Figs. 6–9), indicating that both may share a geochemically identical source. Moreover, the adakitic rocks from the southern side of the IYS yield Nd model ages (T_{DM} = 1.0–1.3 Ga, except for one Mayum sample, which yields 0.5 Ga) similar to those of the adakitic rocks (T_{DM} = 1.1–1.8 Ga) and Early Cretaceous granites and rhyolites (T_{DM} = 1.2–1.5 Ga) in the western Lhasa terrane, also supporting the proposal that all these rocks were derived from the same crustal source.

5.4. Southeastward ductile flow of the mid-lower crust beneath western Lhasa

Geophysical studies have shown that the middle crust below the Lhasa terrane and the High Himalaya range share some similar anomalies, including the bright spots in Southern Tibet among present-day plutons in the middle crust, which are analogous to the Miocene leucogranite plutons exposed farther south in the High Himalaya range (e.g., Chen et al., 1996; Gaillard et al., 2004; Nelson et al., 1996; Unsworth et al., 2005). A model of channel flow in the middle crust has been proposed to explain these phenomena (Beaumont et al., 2001, 2004, 2006; Hodges, 2006; Hodges et al., 2001; Medvedev and Beaumont, 2006; Nelson et al., 1996; Unsworth et al., 2005). Subsequently, King et al. (2007) proposed that the Kuday dykes are the result of partial melting of the Asian plate where it extends south of the IYS as a mid-crustal ductile channel structure beneath Southern Tibet. However, as mentioned above, the Kuday dykes have an adakitic affinity, indicating a source in the lower crust. In addition, the Mayum adakitic rocks (Jiang et al., 2006) were also derived from a lower-crust source at depths greater than 50 km. The geochemical characteristics of adakitic rocks on the south side of the IYS are similar to those of adakitic rocks from the western Lhasa terrane, but different to those from the eastern Lhasa terrane, suggesting that crustal material beneath the eastern Lhasa terrane did not flow southwards below the Himalayas.

Although previous geophysical observations (e.g., Nelson et al., 1996) and the results of geodynamic modeling (e.g., Beaumont et al., 2001, 2006) suggest that channel flow may occur at depths of 20–30 km beneath southern Tibet (i.e., mid-crustal levels), other recent studies suggest that channel flow may also occur in the lower crust, as indicated by widespread high-conductivity layers in the mid-lower crust (e.g., Jin et al., 2010; Wei et al., 2010), a pronounced low-velocity channel that extends from 30 to 70 km depth in the mid-lower crust (e.g., Cotte et al., 1999), and the fact that earthquakes are absent at depths of 30–65 km beneath the Lhasa terrane (e.g., Chen and Yang, 2004; Jackson 2002a, 2002b; Jackson et al., 2004). These findings imply that mid-lower crustal material beneath Southern Tibet is ductile and therefore may take place ductile flow. Moreover, the widespread occurrence of Miocene ultrapotassic and adakitic rocks in the Lhasa terrane, interpreted as melts of metasomatized lithospheric mantle and mafic lower crust, respectively (e.g., Chung et al., 2003, 2005; Williams et al., 2001; Zhao et al., 2009), indicates that Miocene lower crust and lithospheric mantle beneath Southern Tibet were hot and contained melts, which would have favored channel flow within the lower crust.

Combining all the data on the geochemical characteristics of the adakitic rocks on both sides of the IYS, we conclude that the lower crust (and/or middle crust) of the western Lhasa terrane probably extended to the southern side of the IYS via southeastward flow of anatectic mid-lower crustal material along a ductile channel structure during the Miocene (Fig. 11). The geochronological data from high-grade metamorphic and intrusive rocks in the Greater Himalayan Sequence (GHS) beneath and along the Southern Tibetan Detachment System (STDS) indicate that channel flow in the middle crust was

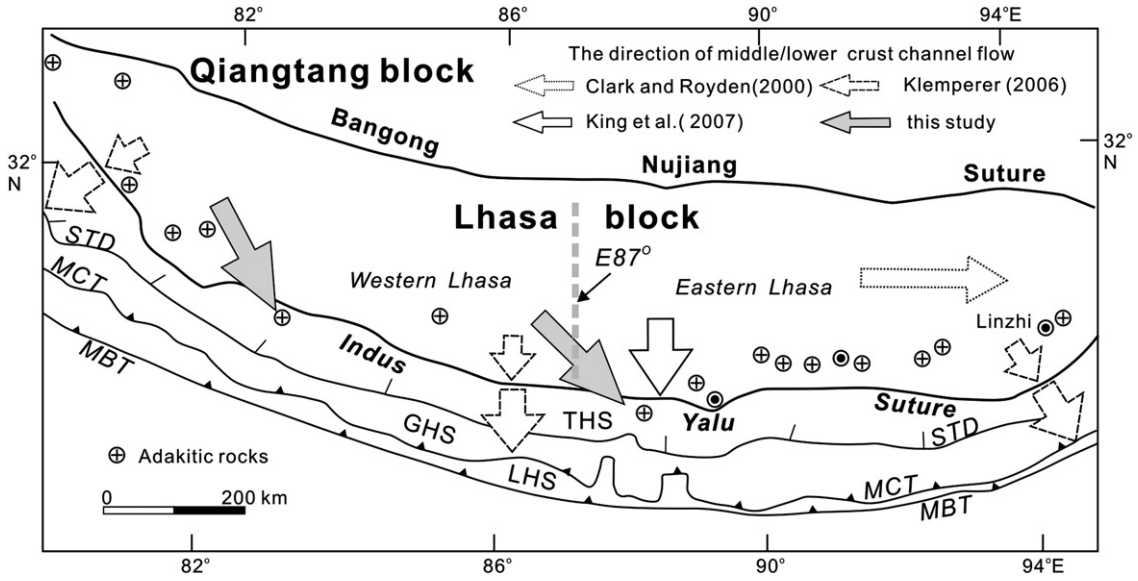

Fig. 11. Suggested directions of middle/lower-crustal channel flow in Southern Tibet, based on Klemperer (2006). STD, Southern Tibetan Detachment; MCT, Main Central Thrust; MBT, Main Boundary Thrust; LHS, Lesser Himalayan Sequence; GHS, Greater Himalayan Sequence; THS, Tethyan Himalayan Sequence.

already in progress by the Early Miocene (e.g., Murphy and Harrison, 1999; Sealer et al., 2003). However, the timing of the onset of southward ductile flow under the Lhasa terrane is unknown, even though this is crucial for characterizing the geodynamic evolution of Southern Tibet. King et al. (2007) suggested that the timing of onset of the southward ductile flow of the Asian material was 12–9 Ma. However, the Mayum adakitic rocks south of the IYS were emplaced at about 17 Ma (Jiang et al., 2006), which suggests that the onset of southeastward ductile flow beneath the western Lhasa terrane may have occurred as early as 17 Ma.

Although Harrison (2006) thought that there exists insufficient evidence for a channel flow of partially molten crust from beneath the Tibetan Plateau during the formation of the Himalayas, the model of crustal channel flow (Beaumont et al., 2001, 2004) is consistent with many observed features of the Himalayan–Tibetan system. For example, geophysical studies have shown that the partially molten middle crust is being extruded southward below Southern Tibet on the south side of the IYS (Nelson et al., 1996; Unsworth et al., 2005), which demonstrates the existence of crustal channel flow beneath Southern Tibet. On the other hand, extensive crustal channel flow beneath the Himalaya area seems unlikely, because of the occurrence of the north-dipping rigid and cold Indian craton, as well as the Karakoram fault that interrupted possible channel flow processes in the western Himalaya (Leech, 2008). Therefore, we suggest that southeastward ductile flow in the mid-lower crust was localized, probably limited to the area immediately south of the IYS. As a result, adakitic rocks are less common on the south side of the IYS than in the southern part of the Lhasa terrane.

6. Conclusions

(1) The geochemical characteristics of Miocene adakitic rocks in the western part of the Lhasa terrane differ from those in the eastern part, indicating contrasting compositions and ages of the lower crust beneath the western and eastern Lhasa terranes.

(2) Miocene adakitic rocks within the Himalayas on the southern side of the IYS have similar geochemical characteristics to those in the western Lhasa terrane, indicating that the adakitic rocks in both areas have a common lower-crustal source.

(3) The occurrence of Miocene adakitic rocks on the southern side of the IYS indicates that mid-lower crust material from beneath the western Lhasa terrane probably extended to beneath the Himalayas via southeastward ductile flow in the mid-lower crust.

Supplementary materials related to this article can be found online at doi:10.1016/j.lithos.2011.05.006.

Acknowledgements

We thank Dr. Zhidan Zhao and one anonymous reviewer together with Lithos Editor-in-Chief Nelson Eby and journal manager Ruud Koole for helpful comments that improved the manuscript. Dr. Bill Griffin and Brent McInnes are thanked for their assistance with zircon U–Pb dating at LA-ICP-MS lab in Australia. This research was supported by the following funding agencies: the Chinese Academy of Sciences (KZCX2-YW-Q04), the Major State Basic Research Program of the People's Republic of China (2009CB421004), the Natural Science Foundation of China (40772046, 40872055, 40930316, 41073033, and 41003018), and the China Geological Survey (1212010818098). This is contribution No. IS -1348 from GIGCAS.

References

Beaumont, C., Jamieson, R.A., Nguyen, M.H., Lee, B., 2001. Himalayan tectonics explained by extrusion of a low-viscosity crustal channel coupled to focused surface denudation. Nature 414, 738–742.

Beaumont, C., Jamieson, R.A., Nguyen, M.H., Medvedev, S., 2004. Crustal channel flows: 1. Numerical models with applications to the tectonics of the Himalayan–Tibetan orogen. Journal of Geophysical Research B06406, 109. doi:10.1029/2003JB002809.

Beaumont, C., Nguyen, M.H., Jamieson, R.A., Ellis, S., 2006. Crustal flow modes in large hot orogens. In: Law, R.D., Searle, M.P., Godin, L. (Eds.), Channel Flow, Ductile Extrusion and Exhumation in Continental Collision Zones: Geological Society, London, Special Publication, 268, pp. 91–145.

Cai, Z.Y., Qiu, R.Z., Xiong, X.L., Huang, G.C., Zhou, S., Meng, X.J., 2005. The adakite-like intrusive rocks characteristics of western Tibet and their prospecting significance. Geotectonica et Metallogenia 29, 491–501 (in Chinese with English abstract).

Chen, W.P., Yang, Z., 2004. Earthquakes beneath the Himalayas and Tibet: evidence for strong lithospheric mantle. Science 304, 1949–1952.

Chen, L., Booker, J., Jones, A., Nong, W., Unsworth, M., Wei, W., Tan, H., 1996. Electromagnetic images of colliding continents: a magnetotelluric survey of the Tsangpo suture zone and surrounding regions. Science 274, 1694–1696.

Chen, J.L., Xu, J.F., Wang, B.D., Kang, Z.Q., Li, J., 2010. Origin of Cenozoic alkaline potassic volcanic rocks at KonglongXiang, Lhasa terrane, Tibetan Plateau: products of partial melting of a mafic lower-crustal source? Chemical Geology 273, 286–299.

Chung, S.L., Liu, D.Y., Ji, J.Q., Chu, M.F., Lee, H.Y., Wen, D.J., Lo, C.H., Lee, T.Y., Qian, Q., Zhang, Q., 2003. Adakites from continental collision zones: melting of thickened lower crust beneath southern Tibet. Geology 31, 1021–1024.
Chung, S.L., Chu, M.F., Zhang, Y., Xie, Y., Lo, C.H., Lee, T.Y., Lan, C.Y., Li, X., Zhang, Y.Q., Wang, Y., 2005. Tibetan tectonic evolution inferred from spatial and temporal variations in post-collisional magmatism. Earth Science Reviews 68, 173–196.
Chung, S.L., Chu, M.F., Ji, J.Q., O'Reilly, S.Y., Pearson, N.J., Liu, D.Y., Lee, T.Y., Lo, C.H., 2009. The nature and timing of crustal thickening in Southern Tibet: geochemical and zircon Hf isotopic constraints from postcollisional adakites. Tectonophysics 477, 36–48.
Clark, M.C., Royden, L.H., 2000. Topographic ooze: building the eastern margin of Tibet by lower crustal flow. Geology 28, 703–706.
Cotte, N., Pedersen, H., Campillo, M., Mars, J., Ni, J.F., Kind, R., Sandvol, E., Zhao, W., 1999. Determination of the crustal structure in southern Tibet by dispersion and amplitude analysis of Rayleigh waves. Geophysical Journal International 138, 809–819.
Coulon, C., Maluski, H., Bollinger, C., Wang, S., 1986. Mesozoic and Cenozoic volcanic rocks from central and southern Tibet: $^{39}Ar/^{40}Ar$ dating, petrological characteristics and geodynamical significance. Earth and Planetary Science Letters 79, 281–302.
Defant, M.J., Drummond, M.S., 1990. Derivation of some modern arc magmas by melting of young subducted lithosphere. Nature 347, 662–665.
Dewey, J.F., Shackleton, R.M., Chang, C.F., Sun, Y.Y., 1988. The tectonic evolution of the Tibetan Plateau. Philosophical Transactions of the Royal Society of London. Series A 327, 379–413.
Ding, L., Kapp, P., Zhong, D.L., Deng, W.M., 2003. Cenozoic volcanism in Tibet: evidence for a transition from oceanic to continental subduction. Journal of Petrology 44, 1833.
Drummond, M.S., Defant, M.J., 1990. A model for trondhjemite–tonalite–dacite genesis and crustal growth via slab melting: Archean to modern comparisons. Journal of Geophysical Research 95, 21503–21521.
Gaillard, F., Scaillet, B., Pichavant, M., 2004. Evidence for present-day leucogranite pluton growth in Tibet. Geology 32, 801–804.
Gao, Y.F., Hou, Z.Q., Kamber, B.S., Wei, R.H., Meng, X.J., Zhao, R.S., 2007a. Adakite-like porphyries from the southern Tibetan continental collision zones: evidence for slab melt metasomatism. Contributions to Mineralogy and Petrology 153, 105–120.
Gao, Y.F., Hou, Z.Q., Kamber, B.S., Wei, R.H., Meng, X.J., Zhao, R.S., 2007b. Lamproitic rocks from a continental collision zone: evidence for recycling of subducted Tethyan oceanic sediments in the mantle beneath southern Tibet. Journal of Petrology 48, 729–752.
Gao, Y.F., Yang, Z.S., Santosh, M., Hou, Z.Q., Wei, R.H., Tian, S.H., 2010. Adakitic rocks from slab melt-modified mantle sources in the continental collision zone of southern Tibet. Lithos 119, 651–663.
Goto, A., Tatsumi, Y., 1996. Quantitative analysis of rock samples by an X-ray fluorescence spectrometer (II). The Rigaku Journal 13, 20–38.
Griffin, W.L., Wang, X., Jackson, S.E., Pearson, N.J., O'Reilly, S.Y., Xu, X.S., Zhou, X.M., 2002. Zircon chemistry and magma mixing, SE China: in-situ analysis of Hf isotopes, Tonglu and Pingtan igneous complexes. Lithos 61, 237–269.
Guo, Z.F., Wilson, M., Liu, J.Q., 2007. Post-collisional adakites in south Tibet: products of partial melting of subduction-modified lower crust. Lithos 96, 205–224.
Harris, N.B.W., Xu, R.H., Lewis, C.L., Hawkesworth, C.J., Zhang, Y.Q., 1988. Isotope geochemistry of the 1985 Tibet Geotraverse, Lhasa to Golmud. Philosophical Transactions of the Royal Society of London. Series A 327, 263–285.
Harrison, T.M., 2006. Did the Himalayan crystallines extrude partially molten from beneath the Tibetan Plateau. In: Law, R.D., et al. (Ed.), Channel flow, ductile extrusion and exhumation of lower-mid crust in continental collision zones: Geological Society, London, Special Publications, 268, pp. 237–254.
Hodges, K.V., 2006. A synthesis of the channel flow-extrusion hypothesis as developed for the Himalayan–Tibetan orogenic system. Geological Society, London, Special Publications 268, 71–90.
Hodges, K.V., Hurtado, J.M., Whipple, K.X., 2001. Southward extrusion of Tibetan crust and its effect on Himalayan tectonics. Tectonics 20, 799–809.
Hou, Z.Q., Gao, Y.F., Qu, X.M., Rui, Z.Y., Mo, X.X., 2004. Origin of adakitic intrusives generated during mid-Miocene east–west extension in southern Tibet. Earth and Planetary Science Letters 220, 139–155.
Hou, Z.Q., Zhao, Z.D.D., Gao, Y.F., Yang, Z.M., Jiang, W., 2006. Tearing and dischronal subduction of the Indian continental slab: evidence from cenozoic Gangdese volcano-magmatic rocks in south Tibet. Acta Petrologica Sinica 22, 761–774 (in Chinese with English abstract).
Jackson, J., 2002a. Strength of the continental lithosphere: time to abandon the jelly sandwich? GSA Today 12, 4–10.
Jackson, J., 2002b. Faulting, flow, and the strength of the continental lithosphere. International Geology Review 44, 39–61.
Jackson, J., Austrheim, H., McKenzie, D., Priestley, K., 2004. Metastability, mechanical strength, and the support of mountain belts. Geology 32, 625–628.
Jiang, W., Mo, X.X., Zhao, C.H., Guo, T.Y., Zhang, S.Q., 1999. Geochemistry of granitoid and its mafic microgranular enclave in Gangdese belt, Qinghai–Xizang Plateau. Acta Petrologica Sinica 15, 89–97 (in Chinese with English abstract).
Jiang, S.H., Nie, F.J., Hu, P., Liu, Y., 2006. 40Ar/39Ar age and geochemical features of the Mayum adakitic porphyry in Tibet. Acta Petrologica Sinica 22, 603–611 (in Chinese with English abstract).
Jin, S., Wei, W.B., Wang, S., Ye, G.F., Deng, M., Tan, H.D., 2010. Discussion of the formation and dynamic signification of the high conductive layer in Tibetan crust. Chinese Journal of Geophysics 53, 2376–2385.
Kay, R.W., 1978. Aleutian magnesian andesites: melts from subducted Pacific Ocean crust. Journal of Volcanology and Geothermal Research 4, 117–132.
Kay, S.M., Ramos, V.A., Marquez, M., 1993. Evidence in Cerro-Pampa volcanic-rocks for slab-melting prior to ridge–trench collision in Southern South-America. Journal of Geology 101, 703–714.
King, J., Harris, N., Argles, T., Parrish, R., Charlier, B., Sherlock, S., Zhang, H.F., 2007. First field evidence of southward ductile flow of Asian crust beneath southern Tibet. Geology 35, 727–730.
Klemperer, S.L., 2006. Crustal flow in Tibet: geophysical evidence for the physical state of Tibetan lithosphere, and inferred patterns of active flow. In: Law, R.D., Searle, M.P., Godin, L. (Eds.), Channel Flow, Ductile Extrusion and Exhumation in Continental Collision Zones: Geological Society, London, Special Publication, 268, pp. 39–70.
Le Bas, M.J., Le Maitre, R.W., Streckeisen, A., Zanettin, B., 1986. A chemical classification of volcanic rocks based on the total alkali-silica diagram. Journal of Petrology 27, 745–750.
Leech, M.L., 2008. Does the Karakoram fault interrupt mid-crustal channel flow in the western Himalayan. Earth and Planetary Science Letters 276, 314–322.
Li, X.H., Liu, D.Y., Sun, M., Li, W.X., Liang, X.R., Liu, Y., 2004. Precise Sm -Nd and U-Pb isotopic dating of the super-giant Shizhuyuan polymetallic deposit and its host granite, Southeast China. Geological Magazine 141, 225–231.
Mahoney, J., Frei, R., Tejada, M., Mo, X., Leat, P., Nagler, T., 1998. Tracing the Indian Ocean mantle domain through time: isotopic results from Old West Indian, East Tethyan, and South Pacific seafloor. Journal of Petrology 39, 1285–1306.
Martin, H., 1986. Effect of steeper Archean geothermal gradient on geochemistry of subduction-zone magmas. Geology 14, 753–756.
Medvedev, S., Beaumont, C., 2006. Growth of continental plateaus by channel injection: models designed to address constraints and thermomechanical consistency. Geological Society, London, Special Publications 268, 147–164.
Miller, C., Schuster, R., Klotzli, U., Frank, W., Purtscheller, F., 1999. Post-collisional potassic and ultrapotassic magmatism in SW Tibet: geochemical and Sr–Nd–Pb–O isotopic constraints for mantle source characteristics and petrogenesis. Journal of Petrology 40, 1399–1424.
Miller, C., Thoni, M., Frank, W., Schuster, R., Melcher, F., Meisel, T., Zanetti, A., 2003. Geochemistry and tectonomagmatic affinity of the Yungbwa ophiolite, SW Tibet. Lithos 66, 155–172.
Mo, X.X., Niu, Y.L., Dong, G.C., Zhao, Z.D., Hou, Z.Q., Su, Z., Ke, S., 2008. Contribution of syncollisional felsic magmatism to continental crust growth: a case study of the Paleogene Linzizong volcanic succession in southern Tibet. Chemical Geology 250, 49–67.
Murphy, M.A., Harrison, T.M., 1999. Relationship between leucogranites and the Qomolangma detachment in the Rongbuk valley, South Tibet. Geology 27, 831–834.
Murphy, M.A., Yin, A., Harrison, T.M., Durr, S.B., Chen, Z., Ryerson, F.J., Kidd, W.S.F., Wang, X., Zhou, X., 1997. Did the Indo-Asian collision alone create the Tibetan plateau? Geology 25, 719–722.
Nelson, K.D., Zhao, W.J., Brown, L.D., Kuo, J., Che, J.K., Liu, X.W., Klemperer, S.L., Makovsky, Y., Meissner, R., Mechie, J., Kind, R., Wenzel, F., Ni, J., Nabelek, J., Chen, L.S., Tan, H.D., Wei, W.B., Jones, A.G., Booker, J., Unsworth, M., Kidd, W.S.F., Hauck, M., Alsdorf, D., Ross, A., Cogan, M., Wu, C.D., Sandvol, E., Edwards, M., 1996. Partially molten middle crust beneath southern Tibet: synthesis of project INDEPTH results. Science 274, 1684–1688.
Nomade, S., Renne, P.R., Mo, X.X., Zhao, Z.D., Zhou, S., 2004. Miocene volcanism in the Lhasa block, Tibet: spatial trends and geodynamic implications. Earth and Planetary Science Letters 221, 227–243.
Owens, T.J., Zandt, G., 1997. Implications of crustal property variations for models of Tibetan plateau evolution. Nature 387, 37–43.
Petford, N., Atherton, M., 1996. Na-rich partial melts from newly underplated basaltic crust: the Cordillera Blanca Batholith, Peru. Journal of Petrology 37, 1491–1521.
Qu, X.M., Hou, Z.Q., Li, Z.Q., 2003. $^{40}Ar/^{39}Ar$ ages of porphyries from the Gangdese porphyry Cu belt in south Tibet and implication to geodynamic setting. Acta Geologica Sinica 20, 355–366.
Scharer, U., Xu, R.H., Allegre, C.J., 1984. U–Pb geochronology of Gangdese (Transhimalaya) plutonism in the Lhasa–Xigaze region, Tibet. Earth and Planetary Science Letters 69, 311–320.
Sealer, M.P., Simpson, R.L., Law, R.D., Parrish, R.R., Waters, D.J., 2003. The structural geometry, metamorphic and magmatic evolution of the Everest massif, High Himalaya of Nepal-south Tibet. Journal of the Geological Society, London 160, 345–366.
Song, Q., 1999. Geochemical features of the volcanic rocks of Linzizong group in Cuoqin Basin. Journal of Geomechanics 5, 65–70 (in Chinese with English abstract).
Stern, C.R., Kilian, R., 1996. Role of the subducted slab, mantle wedge and continental crust in the generation of adakites from the Andean Austral Volcanic Zone. Contributions to Mineralogy and Petrology 123, 263–281.
Sun, S.S., McDonough, W.F., 1989. Chemical and isotopic systematics of oceanic basalts: implications for mantle composition and processes. Geological Society, London, Special Publication 42, 313–345.
Turner, S., Arnaud, N., Liu, J.Q., Rogers, N., Hawkesworth, C., Harris, N., Kelley, S., Calsteren, P.V., Deng, W., 1996. Post-collision, shoshonitic volcanism on the Tibetan plateau: implications for convective thinning of the lithosphere and the source of ocean island basalts. Journal of Petrology 37, 45–71.
Unsworth, M.J., Jones, A.G., Wei, W., Marquis, G., Gokarn, S.G., Spratt, J.E., Team, I.M., 2005. Crustal rheology of the Himalaya and Southern Tibet inferred from magnetotelluric data. Nature 438, 78–81.
Wei, G.J., Liang, X.R., Li, X.H., Liu, Y., 2002. Precise measurement of Sr isotopic composition of liquid and solid base using (LP)MC-ICPMS. Geochimica 31, 295–299. (in Chinese with English abstract).
Wei, W.B., Jin, S., Ye, G.F., Deng, M., Jing, J.E., Unsworth, M., Jones, A.G., 2010. Conductivity structure and rheological property of lithosphere in Southern Tibet inferred from super-broadband magnetotelluric sounding. Science in China 53, 189–192.

Williams, I.S., Buick, I.S., Cartwright, I., 1996. An extended episode of early Mesoproterozoic metamorphic fluid flow in the Reynold Region, central Australia. Journal of Metamorphic Geology 14, 29–47.
Williams, H.M., Turner, S.P., Kelley, S.P., Harris, N.B.W., 2001. Age and composition of dikes in Southern Tibet: new constraints on the timing of east–west extension and its relationship to postcollisional volcanism. Geology 29, 339–342.
Williams, H.M., Turner, S.P., Pearce, J.A., Kelley, S.P., Harris, N.B.W., 2004. Nature of the source regions for post-collisional, potassic magmatism in southern and northern Tibet from geochemical variations and inverse trace element modelling. Journal of Petrology 45, 555–607.
Wu, X.L., Feng, Y., Huang, J.P., 2005. Geochemical characteristics of Nianbo Formation at Cuoqin County, Tibet and its geotectonic significance. Journal of East China Institute of Technology 28, 5–11 (in Chinese with English abstract).
Xiao, L., Wang, C.Z., Pirajno, F., 2007. Is the underthrust Indian lithosphere split beneath the Tibetan Plateau? International Geology Review 49, 90–98.
Xiong, X.L., Adam, J., Green, T.H., 2005. Rutile stability and rutile/melt HFSE partitioning during partial melting of hydrous basalt: implications for TTG genesis. Chemical Geology 218, 339–359.
Xu, J.F., Castillo, P.R., 2004. Geochemical and Nd–Pb isotopic characteristics of the Tethyan asthenosphere: implications for the origin of the Indian Ocean mantle domain. Tectonophysics 393, 9–27.
Xu, J.F., Shinjo, R., Defant, M.J., Wang, Q.A., Rapp, R.P., 2002. Origin of Mesozoic adakitic intrusive rocks in the Ningzhen area of east China: partial melting of delaminated lower continental crust? Geology 30, 1111–1114.
Xu, X.S., Deng, P., O'Reilly, S.Y., Griffin, W.L., Zhou, X.M., Tan, Z.Z., 2003. Single zircon LAM-ICPMS U–Pb dating of Guidong complex (SE China) and its petrogenetic significance. Chinese Science Bulletin 48, 1892–1899.
Xu, W.C., Zhang, H.F., Guo, L., Yuan, H.L., 2010. Miocene high Sr/Y magmatism, south Tibet: product of partial melting of subducted Indian continental crust and its tectonic implication. Lithos 114, 293–306.
Yin, A., Harrison, T.M., 2000. Geologic evolution of the Himalayan–Tibetan orogen. Annual Reviews of Earth and Planetary Science 28, 211–280.
Yue, Y.H., Ding, L., 2006. $^{40}Ar/^{39}Ar$ geochronology, geochemical characteristics and genesis of the Linzhou basic dikes, Tibet. Acta Petrologica Sinica 22, 855–866 (in Chinese with English abstract).
Zhang, S.Q., 1996. Mesozoic and Cenozoic volcanism in central Gangdese: implications for lithospheric evolution of the Tibetan Plateau. Unpublished Ph.D. thesis in Beijing. China University of Geosciences (in Chinese with English abstract).
Zhang, H.F., Harris, N., Parrish, R., Kelley, S., Zhang, L., Rogers, N., Argles, T., King, J., 2004. Causes and consequences of protracted melting of the mid-crust exposed in the North Himalayan antiform. Earth and Planetary Science Letters 228, 195–212.
Zhang, S.Q., Mahoney, J.J., Mo, X.X., Ghazi, A.M., Milani, L., Crawford, A.J., Guo, T.Y., Zhao, Z.D., 2005. Evidence for a widespread Tethyan upper mantle with Indian-Ocean-type isotopic characteristics. Journal of Petrology 46, 829–858.
Zhao, W.J., Nelson, K.D., 1993. Deep seismic-reflection evidence for continental underthrusting beneath Southern Tibet. Nature 366, 557–559.
Zhao, Z.D., Mo, X.X., Nomade, S., Renne, P.R., Zhou, S., Dong, G.C., Wang, L.L., Zhu, D.C., Liao, Z.L., 2006. Post-collisional ultrapotassic rocks in Lhasa block, Tibetan Plateau Spatial and temporal distribution and its' implications. Acta Petrologica Sinica 22, 787–794 (in Chinese with English abstract).
Zhao, Z.D., Mo, X.X., Dilek, Y., Niu, Y.L., DePaolo, D.J., Robinson, P., Zhu, D.C., Sun, C.G., Dong, G.C., Zhou, S., Luo, Z.H., Hou, Z.Q., 2009. Geochemical and Sr–Nd–Pb–O isotopic compositions of the post-collisional ultrapotassic magmatism in SW Tibet: petrogenesis and implications for India intra-continental subduction beneath southern Tibet. Lithos 113, 190–212.
Zhou, H.W., Murphy, M.A., 2005. Tornographic evidence for wholesale underthrusting of India beneath the entire Tibetan plateau. Journal of Asian Earth Sciences 25, 445–457.
Zhu, D.C., Mo, X.X., Niu, Y.L., Zhao, Z.D., Wang, L.Q., Liu, Y.S., Wu, F.Y., 2009. Geochemical investigation of Early Cretaceous igneous rocks along an east–west traverse throughout the central Lhasa Terrane, Tibet. Chemical Geology 228, 298–312.